Taylor & Francis
Taylor & Francis Group

Far-Field Patterns from Dye-Doped Planar-Aligned Nematic Liquid Crystals Under Nanosecond Laser Irradiation

Svetlana G. Lukishova
Nick Lepeshkin*
Robert W. Boyd
The Institute of Optics, University of Rochester, Rochester,
New York, USA

Kenneth L. Marshall
Laboratory for Laser Energetics, University of Rochester, Rochester,
New York, USA

High-definition patterns were observed under 10-Hz-pulse-repetition-rate, nanosecond laser irradiation of azodye-doped planar-nematic liquid crystal layers at incident intensities $I \sim 5$–$10\,MW/cm^2$ in a single beam configuration and without any feedback involved. An incident polarization parallel to the nematic director was used. Under periodic pulsed laser irradiation, far-field beam patterns at the output of a dye-doped liquid crystal layer changed kaleidoscopically from rings and stripes to multiple hexagons. This pattern-formation regime had a buildup time of several seconds to minutes. We explain the observed effect by diffraction of the laser beam on light-induced micrometer-size inhomogeneities inside the liquid crystal layer with absorption and refraction properties different from the surrounding area. Possible mechanisms of the formation of the inhomogeneities are discussed.

1. INTRODUCTION

Single-beam, feedback-free patterns in the far-field have been reported for nanosecond laser irradiation of planar-aligned liquid crystals (LCs) in Refs. [1,2]. Both two-photon absorbing [1] and dye-doped liquid crystals [2] have been used in an irradiation geometry with the incident polarization parallel to the nematic director. This geometry does not permit the first-order electric field induced reorientation of the nematic molecules [3], allowing us to exclude its contribution to the nonlinear response. Cumulative effects connected with light absorption of pulsed laser radiation in liquid crystals [1] and laser-induced local heating of material were responsible for appearance of different patterns with buildup times ranging from several seconds to minutes, in the form of rings [1], a "dark" spot [1], and a four-leaf-clover (a Maltese-like cross) [1,2] from an initial Gaussian spatial intensity distribution. In addition, the appearance of the polarization component perpendicular to the nematic director was reported [2]. The experiments described in the present paper were performed under the same experimental conditions as those in Ref. [2], but at higher incident intensities. Under these conditions, the appearance of new far-field beam patterns was observed in the form of stripes, hexagons and rings for the polarization component parallel to the nematic director. These results could be potentially useful for photonic devices based on thin layers of doped LCs absorbing repetitively pulsed, focused laser radiation, for instance, optical power limiters, 1-D photonic-band-gap chiral nematic LC lasers [4,5] and LC single-photon sources [6,7].

The structure of this paper is as follows. Section 2 describes the experimental setup and planar-aligned LC-layer scheme used in the experiments. Section 3 describes the characterization of our materials and LC-cell fabrication. In Section 4, the results on polarization-dependent spatial pattern formation in laser beam cross-section are reported. Section 5 presents the polarizing microscope images of LC samples after switching off the incident laser radiation. In Section 6, the possible mechanisms producing the described phenomena are discussed. Section 7 concludes the paper.

2. EXPERIMENTAL SETUP

A 0.532-μm laser beam with a pulse duration of $\sim$20–26 ns and pulse repetition rate 10 Hz was focused by a 24-cm-focal-length lens into the

dye-doped, planar-aligned nematic LC cell. The incident polarization was parallel to the orientation of the LC molecular director. The beam diameter in the focus was $\sim 150\,\mu$m at the 1/e level. Further details of the experimental setup could be found in Ref. [2].

The far-field patterns were recorded from a screen by a video camera onto magnetic tape from which the spatial intensity distribution for each pulse was digitized afterwards.

3. LIQUID CRYSTAL CELL PREPARATION

The nematic LC mixture E7 doped with the azodye "Oil Red O" (Fig. 1) with a 1.5% weight-concentration was used for filling the LC cells. E7 was supplied by EM-Industries; Oil Red O was supplied by Sigma-Aldrich.

Planar-aligned nematic LC-layers were prepared using buffing techniques on Nylon 6/6 alignment layers on Soda-Lime-glass plates of size $2.5\,cm \times 2.5\,cm \times 0.3\,cm$. Glass-bead-spacers mixed with an UV-epoxy provided cell thicknesses between 10 and 20 μm. Coating the substrates by Nylon 6/6, buffing, cell assembly, and filling the cells with LC were carried out in a clean room. UV-cured epoxy was used for sealing the cells.

Note, that the dye used for doping liquid crystals was dichroic. Cell transmittance at low incident intensities was $\sim 1\%$ for an incident polarization parallel to the nematic director, and ~ 10–15% for the perpendicular polarization.

4. FAR-FIELD BEAM SPATIAL PATTERNS

As reported in Ref. [2], at incident intensities $I \sim 1$–$5\,MW/cm^2$ several interesting phenomena are observed during repetitive illumination of LC-cells by a focused laser beam with 10-Hz pulse-repetition rate, for time periods of *several seconds* to *several minutes*. These phenomena include the following:
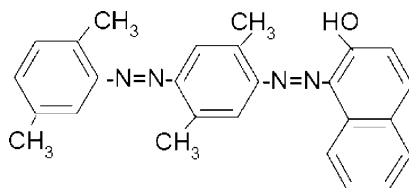

FIGURE 1 Molecular structure of azodye Oil Red O.

　　　　　　　　　　　　　　S. G. Lukishova et al.

- A polarization component *perpendicular* to the nematic director appeared after the beam passed through the nematic layer. Simultaneously, a several-fold increase in cell transmission was observed. The effect was attributed to the trans/cis photo-induced izomerization of the azo-dye molecules.
- Following that, *stable* far-field patterns appeared in the beam cross-section, possibly as the result of heat-flow [8] and/or flow-reorientational [9,10] birefringence:
  1. The *perpendicular* polarization component took on the far-field form of an optical four-leaf clover (Maltese-like cross). The bright axes of the cross were oriented at 45° to the incident polarization;
  2. The incident, *parallel* polarization component evolved into the far-field pattern in the form of a ring with a bright spot inside;
- *Stable* patterns existed for more than one hour of irradiation, but disappeared after switching the laser to a 5-Hz repetition rate.

At the higher-incident-intensities regime, which is the subject of the present paper ($I \sim 5$–$10\,\mathrm{MW/cm^2}$), new kind of high-definition patterns developed with a buildup time of several seconds to minutes and only for the polarization component *parallel* to the nematic director. Figure 2 shows the beam cross-sections of the two spatially separated
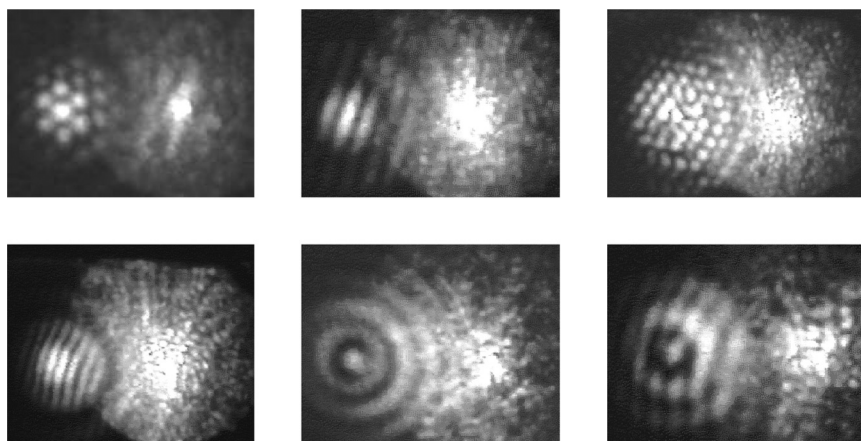

FIGURE 2 Representative selection of far-field spatial patterns at incident intensities ~ 5–$10\,\mathrm{MW/cm^2}$ for the polarization component parallel to the director (left side of each image) and for the induced, perpendicular polarization component (right side of each image). A Glan prism was used to separate the two polarizations.
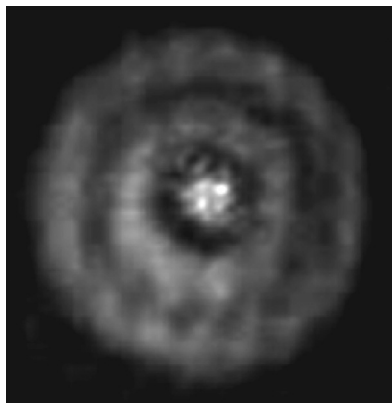
FIGURE 3 Far-field pattern of two polarization components with four-leaf-clover pattern of the "perpendicular" polarization component overlapped with the fringes of the "parallel" polarization component.

polarization components both incident and induced (using a Glan-prism) overlapping in the center. The left side of the images depicts *the parallel-polarization* (incident) component; the right side – *the perpendicular-polarization* (induced) component. The optical four-leaf-clover of the *perpendicular-polarization* component [2] almost always became smeared into a random speckle pattern with a bright spot in the center (see the right side of the images). At times, it did not disappear completely, although its contrast diminished (see Fig. 2, central top image and Fig. 3 obtained without the Glan prism). At the same time, *the parallel-polarization* component developed a high-definition pattern that kaleidoscopically changed from pulse to pulse from rings and stripes to multiple hexagons (see left side of the Fig. 2 images). The patterns disappeared after switching the laser to a 5-Hz repetition rate.

Interestingly, we observed hexagon/stripes/rings patterns in non-oriented nematic LCs and isotropic liquids doped with nondichroic dyes as well, but the stability of the pattern formation in all these experiments was lower than that for dichroic azodye-doped planar-nematic LCs.

5. OPTICAL MICROSCOPE IMAGES OF LIQUID CRYSTAL SAMPLES

Examination of the LC cells by optical polarizing microscopy after laser action showed no changes in planar alignment in most samples. However, in some samples, one, two, or three spots with destroyed alignment
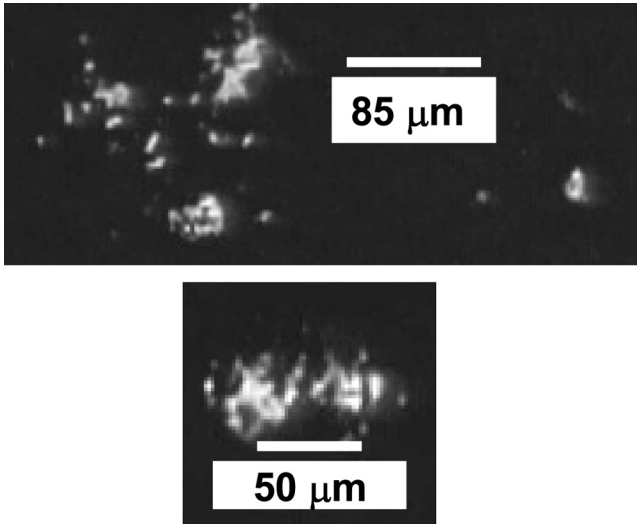
FIGURE 4 Optical polarizing microscope images of planar-aligned liquid crystal cells after laser irradiation, showing one/two/three spots of destroyed planar alignment.

can be seen very clearly. Figure 4 shows a representative polarizing microscope images of an Oil Red O-doped planar-nematic LC cell with several spots where the planar alignment was destroyed. The dimensions of these spots were $\sim$12–30 μm with $\sim$50–90 μm distance between them.

Near-field images of the laser-beam cross-section during the pulsed laser action showed kaleidoscopic changes from one to two and three spots patterns with dimensions $\sim$5–15 μm and distance between spots $\sim$35–70 μm.

6. MECHANISM OF THE HEXAGONAL/STRIPES/RINGS FAR-FIELD PATTERNS

We explain the observed hexagonal/stripes/rings patterns in the far-field by the diffraction of the laser beam on light-induced one/two/three or more several-micron-size "drops" with absorption and/or refraction properties different from the surrounding material. The patterns' ring structure can be attributed to the diffraction of laser light at the sharp edge of the "drops". The variation in the "drop" numbers in the focal region, their size, the distance between them, and the gradient of transmittance inside the drop define the enormous variety of patterns we observed.

The observation of high-definition hexagonal/stripes/rings patterns only for the "parallel" polarization component can be explained by the highly dichroic dye used for this experiment: cell transmittance was an order of magnitude higher for the "perpendicular" polarization component than for the "parallel" polarization component. Hexagonal/ stripes/rings patterns' low contrast makes them invisible for the "perpendicular" polarization component. Only a four-leaf-clover pattern can be seen in this component because of its existence's connection with another mechanism – the aberrations of the laser beam in heat-flow and/or flow-reorientational birefringent media.

The following light-induced mechanisms which can contribute to the creation of "drops" in dye-doped LC-cells will be discussed next: nematic/isotropic phase transition, thermal diffusion (Soret effect) and electrostriction.

6.1. Nematic/Isotropic Phase Transition

The maximum instantaneous temperature during a single pulse can be calculated as $T_{inst} = T_{room} + \varepsilon/\rho S h c_p$. At an incident intensity of $5\,MW/cm^2$, absorbed energy $\varepsilon \sim 18\,\mu J$, pulse duration 20 ns, cross-section $S = \pi(75\,\mu m)^2$; layer thickness h = 10 μm; density $\rho = 1\,g/cm^3$; 3; heat capacity $c_p = 1.92\,J/gK$, $T_{inst} = T_{room} + 53°C$ which is above the nematic/isotropic liquid phase transition temperature $T_c \sim 60°C$.

Figure 5 shows optical microscope images of a phase nucleation in a dye-doped LC cell used in our beam-pattern-formation experiments. The LC-cell was heated inside a Mettler hot stage with 0.1°C heating
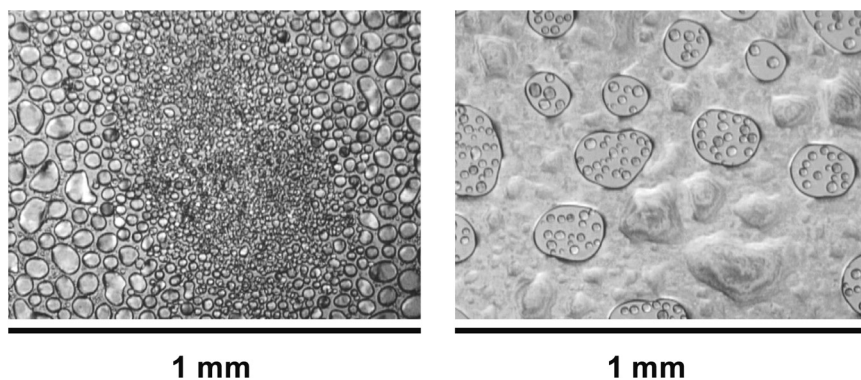

1 mm **1 mm**

FIGURE 5 Optical microscope images of phase nucleation in Oil-Red-O-doped nematic mixture E7 near the nematic/isotropic liquid phase transition (T = 58°C): left – heating, right – cooling of the cell.

steps. No laser radiation was used. Drops of isotropic liquid with sizes ranging from several to hundred microns existed inside the nematic material at $\Delta T = 1$–$2°C$ below the nematic/isotropic phase transition.

The existence of phase nucleation near the nematic/isotropic phase transition of undoped nematic mixtures in a form of multiple isotropic drops was reported in Ref. [11]. Diffraction of a low power density, cw probe beam on isotropic drops created by heating in the oven to the phase-transition-temperature showed a far-field, small-scale hexagonal patterns similar to some of the hexagonal patterns observed in our experiments.

Diffraction by a single, isotropic drop inside the nematic LC created by localized heating of the material above T_c was reported for CW-laser-irradiation in Refs. [12] and [13].

6.2. Soret Effect and Electrostriction

Two other processes can lead to creation of several-micron-size inhomogeneities: thermodiffusion (Soret effect) and electrostriction [14–17]. Even a small, light-induced temperature gradient results in a concentration gradient due to thermodiffusion. These concentration variations, which are responsible for large optical nonlinearities in some systems could also induce phase separation. Such light-induced phase separation with nucleation and trapping of droplets in the laser beams in a binary liquid mixture was reported in Ref. [17]. While thermal diffusion is the main mechanism which causes motion and redistribution of strongly absorbing dye molecules in the electromagnetic field of the light beam, the electrostriction forces resulting from the transverse beam-intensity modulation may still have an effect on the redistribution of dye molecules in liquids.

In our experiments, phase separation of the dye from the liquid with two or several concentration inhomogeneities within the focal area, may have occured. In some experiments, we observed, after irradiation, the dye-drop adsorption onto the substrate. For cw irradiation, similar light-induced dye adsorption from the liquid crystal host was reported in Ref. [18].

7. CONCLUSION

The interaction of 20-ns-duration, 10-Hz-pulse-repetition-rate laser pulses at 532-nm wavelength with a planar-aligned, azodye-doped, nematic liquid crystal layer has been studied for incident polarization *parallel* to the nematic director. At high-intensities ($I \sim 5$–$10\,MW/cm^2$), high-definition patterns in the form of hexagons, stripes and rings

were observed only for the polarization component *parallel* to the nematic director. Diffraction of laser beam on light-induced several-micron-size "drops" with absorption and/or refraction properties different from the surrounding material is responsible for the variety of hexagonal/stripes/rings patterns. Several mechanisms may contribute to the creation of such "drops", for instance, laser induced nematic/isotropic liquid phase transition, the Soret effect, and electrostriction.

REFERENCES

[1] Lukishova, S. G. (2000). *J. Nonl. Opt. Phys. & Mater.*, *9*(3), 365.

[2] Lukishova, S. G., Boyd, R. W., Lepeshkin, N., & Marshall, K. L. (2002). *J. Nonl. Opt. Phys. & Mater.*, *11*(4), 341.

[3] Khoo, I.-C. (1995). *Liquid Crystals, Physical Properties and Nonlinear Optical Phenomena*, John Wiley & Sons: New York.

[4] Il'chishin, I. P., Tikhonov, E. A., Tishchenko, V. G., & Shpak, M. T. (1980). *JETP Lett.*, *32*, 24.

[5] Kopp, V. P., Fan, B., Vithana, H. K. M., & Genack, A. Z. (1998). *Opt. Lett.*, *23*, 1707.

[6] Lukishova, S. G., Schmid, A. W., McNamara, A. J., Boyd, R. W., & Stroud, C. R. Jr. (2003). *IEEE J. Selected Topics in Quant. Electron.*, Spec. Issue on Quantum Internet Technologies, *9*, No. 6, 1512.

[7] Lukishova, S. G., Schmid, A. W., Supranowitz, C. M., Lippa, N., McNamara, A. J., Boyd, R. W., & Stroud, C. R. Jr. (2004). *J. Modern Opt.*, Spec. Issue on Single Photon: Detectors, Applications, and Measurement Methods, *51*(9–10), 1535.

[8] Eichler, R., Macdonald, R., Eichler, H. J., Hess, S., & Sonnet, A. M. (1999). *Phys. Rev.*, *E60*, 1792.

[9] Khoo, I. C., Lindquist, R. G., Michael, R. R., Mansfield, R. J., & LoPresti, P. (1991). *J. Appl. Phys.*, *69*, 3853.

[10] Eichler, H. J. & Macdonald, R. (1991). *Phys. Rev. Lett.*, *67*, 2666.

[11] Zolot'ko, A. S. & Kitaeva, V. F. (1995). *JETP Lett.*, *62*, 124.

[12] Volterra, V. & Wiener-Avnear, E. (1975). *Appl. Phys. E*, *6*, 257.

[13] Bloisi, F., Vicari, L., Simoni, F., Cipparrone, G., & Umeton, C. (1988). *J. Opt. Soc. Am.*, *B5*, 2462.

[14] Eichler, H. J., Günter, P., & Pohl, D. W. (1986). *Laser-Induced Dynamic Gratings*, Springer-Verlag: Berlin, 136.

[15] Tabiryan, N. V. (1999). *Entropie*, *217*, 5.

[16] Tabiryan, N. V. & Luo, W. (1998). *Phys. Rev. E*, *57*, 4431.

[17] Delville, J. P., Lalaude, C., Freysz, E., & Ducasse, A. (1994). *Phys. Rev. E*, *49*, 4145.

[18] Voloschenko, D. & Lavrentovich, O. (1999). *J. Appl. Phys.*, *86*, 4843.